Supplementary Material

1 Schematic Diagram of the Experimental and Numerical Models.

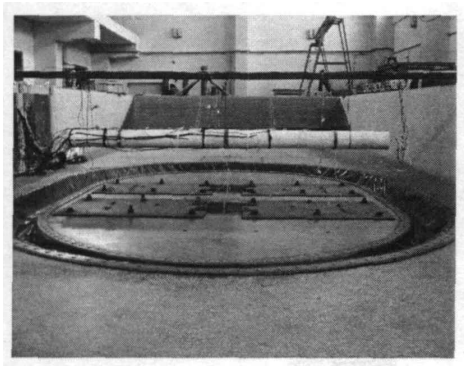

(a)Empty water pool, shaking table and SFTmodel

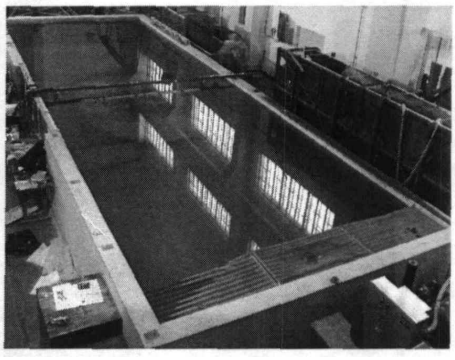

(b)Water filling pool, shaking table and SFT model

Figure S1. Schematic Diagram of the Experimental(Sun and Chen (2008,2012))

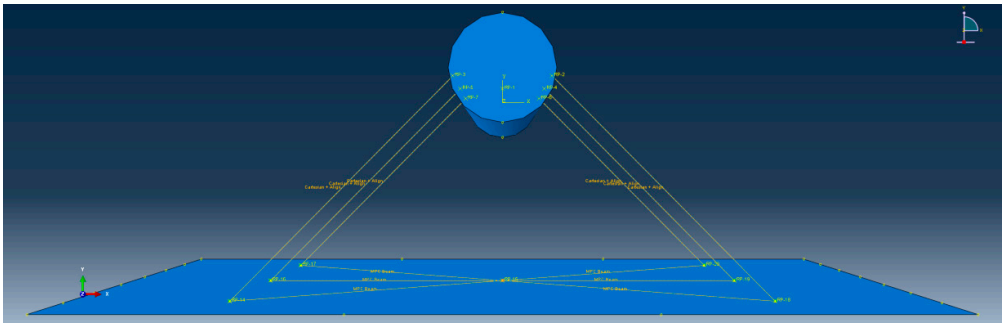

(a)

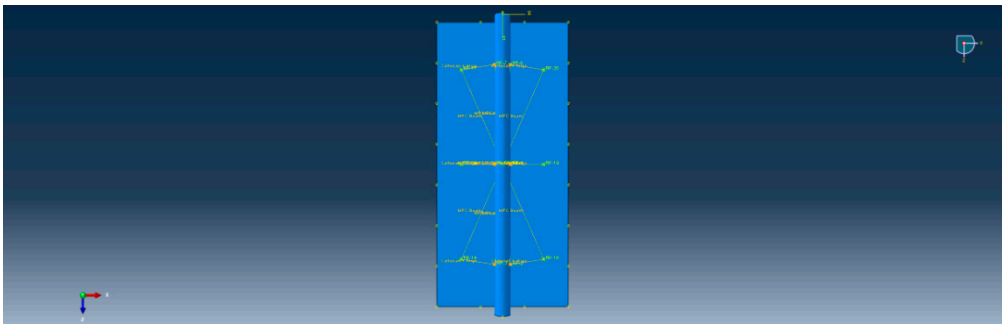

(b)

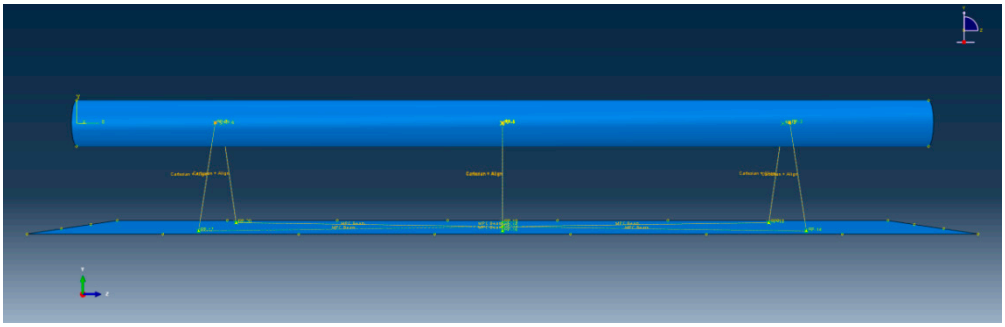

(c)

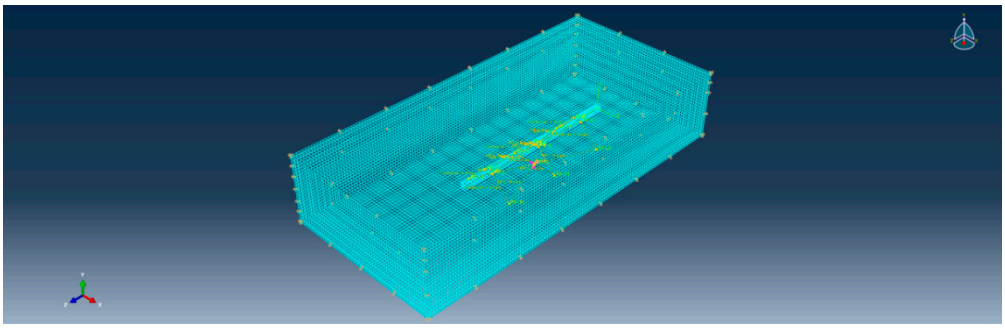

(d)

Figure S2. Schematic Diagram of Numerical Models.

2 Numerical simulation of Circular cylinder flow

This study simulates flow around a cylinder using the experimental setup detailed in reference (Xiao S. 2020) entitled "Drop-tower Microgravity Granular Cylinder Towing Experiment." The experimental apparatus and model dimensions are illustrated in Figure 1.1. The specific model configuration parameters include: treating the cylinder as a rigid body with input for rotational moments of inertia in all directions, modeling the fluid as Eulerian with a density of 1000 kg/m³, viscosity of 0.001 Pa·s, and speed of sound at 1480 m/s. The free surface of the fluid is applied at the top, while the bottom and sides employ smooth boundaries with velocities set to 0. The top of the cylinder is released with a horizontal degree of freedom, while other degrees of freedom are constrained. The contact between the cylinder and the fluid is defined as a smooth, hard contact, meaning no mutual penetration is allowed in the normal direction, and there is zero tangential friction. The model, as depicted in Fig.S3, is subjected to different horizontal velocities (Vx) applied to the top of the cylinder for computational analysis.

(a)Experimental Apparatus (b)Numerical Model of the Experimental Setup

Figure S3. Schematic Diagram of the Experimental and Numerical Models.

3 Velocity Field Contour Maps at Different Stages of the Two-Way Fluid-Structure Coupling Model

The Fig.S4 illustrates the velocity field cloud diagram of the tie rod at various stages during its movement process. Notably, as the tie rod traverses through the fluid at a specific velocity, discernible alterations occur in the velocity field of both the tie rod and the surrounding fluid. This observation signifies a clear interaction between the tie rod and the fluid during their relative movement, thereby establishing a bidirectional fluid-structure coupling calculation model.

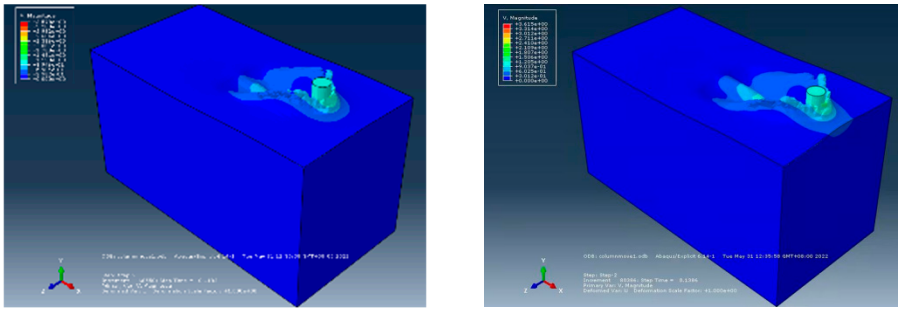

(a) (b)

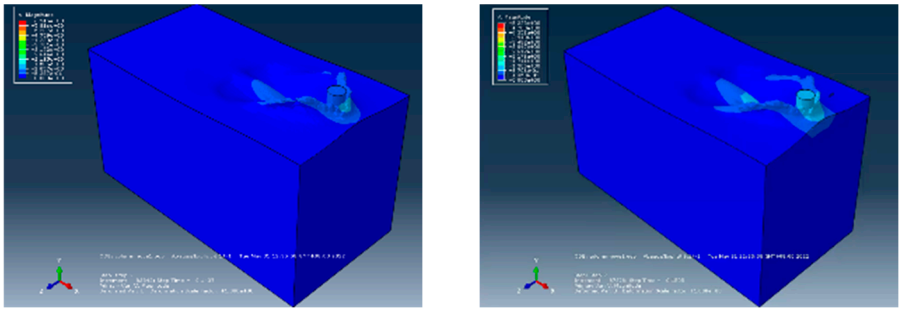

(c) (d)

Figure S4. Velocity field cloud images at different stages of bidirectional fluid-structure coupling of the model

4 Displays simulated and empirical solutions of drag forces on a cylinder at various Reynolds numbers.

Table S1. Comparison of the empirical and simulated drag force calculation results (where V represents the horizontal velocity of the column).

V (m/s)	C_D	*Re*	Drag force Empirical solutions （N/m）	Drag force simulated solutions (N/m)	Relative error%
0.01	1.18	200	0.00118	0.00144	22
0.05	1	1000	0.025	0.031	24
0.1	0.91	2000	0.091	0.11	20.9
0.2	0.92	4000	0.368	0.376	2.2
0.5	1.08	10000	2.7	2.9	7.4
1	1.12	20000	11.2	10.5	6.3
2	1.13	40000	45.2	44.4	1.77
5	1.1	100000	275	256.2	6.8
10	0.97	200000	970	984.9	1.53

Relative error =| simulated solution - empirical solution |/ empirical solution, the value of C_D is read from Fig.4

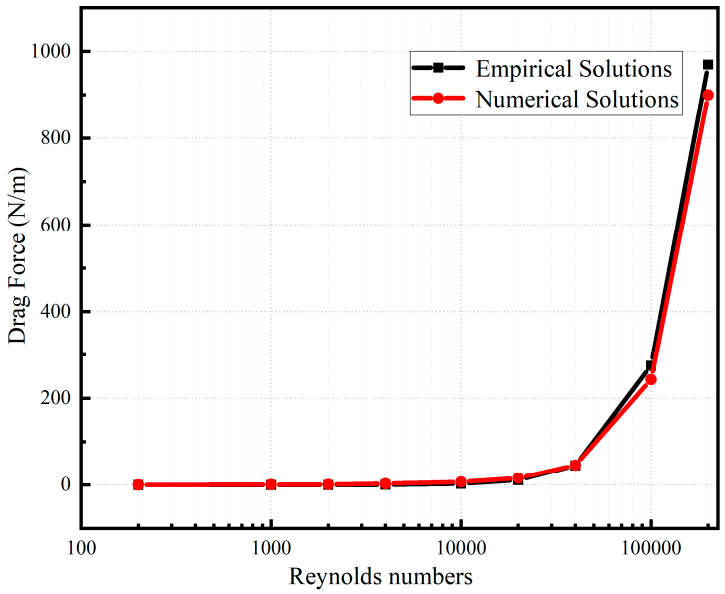

Figure S5. Comparison of numerical and empirical drag force solutions

5 CEL Motion Equations

5.1 Fluid Motion Equations (Eulerian Equations):

The Eulerian equations describe the motion of the fluid, typically in the form of the Navier-Stokes equations. For incompressible fluids, the Navier-Stokes equations (Noh,1964) can be written as:

Mass conservation equation:

$$\frac{\partial \rho}{\partial t} + \nabla \cdot (\rho \mathbf{u}) = 0 \tag{1}$$

Momentum conservation equation:

$$\frac{\partial (\rho \mathbf{u})}{\partial t} + \nabla \cdot (\rho \mathbf{u}\mathbf{u}) = -\nabla p + \nabla \cdot \tau + \rho \mathbf{g} \tag{2}$$

Here, ρ is the density, $\mathbf{u}$ is the velocity vector, p is the pressure, τ is the stress tensor, and $\mathbf{g}$ is the gravitational acceleration vector.

The stress tensor τ in the equation represents the shear stress tensor. For a Newtonian fluid, the shear stress tensor can be expressed through the viscous stress term:

$$\tau = \mu(\nabla \mathbf{u} + (\nabla \mathbf{u})^{\mathrm{T}}) \tag{3}$$

Here, μ is the dynamic viscosity coefficient, and $\nabla \mathbf{u}$ is the velocity gradient.

Under the assumption of incompressible flow, the momentum conservation equation simplifies to:

$$\frac{\partial \mathbf{u}}{\partial t} + (\mathbf{u} \cdot \nabla)\mathbf{u} = -\frac{1}{\rho}\nabla p + \nu \nabla^2 \mathbf{u} + \mathbf{g} \tag{4}$$

Here, ν is the kinematic viscosity.

In the context of the Navier-Stokes equations, which govern fluid dynamics, the pressure term arises from internal forces within the fluid. This includes contributions from both the static component, associated with hydrostatic pressure, and the dynamic component, associated with the motion of the fluid. The total pressure (p) can be expressed using a state equation. For incompressible fluids, a commonly used state equation is:

$$p = p_0 + \frac{1}{2}\rho|\mathbf{u}|^2 \tag{5}$$

Here, p_0 represents the static pressure, ρ is the fluid density, and $\mathbf{u}$ is the fluid velocity vector.

Substituting the state equation (5), the momentum conservation equation can be rewritten as:

$$\frac{\partial \mathbf{u}}{\partial t} + (\mathbf{u}\cdot\nabla)\mathbf{u} = -\frac{1}{\rho}\nabla(p_0 + \frac{1}{2}\rho|\mathbf{u}|^2) + \nu\nabla^2\mathbf{u} + \mathbf{g} \tag{6}$$

This represents the momentum conservation equation with the consideration of the total pressure term. The equation describes fluid motion, including the influence of both static and dynamic pressure within the fluid. It serves as a fundamental equation for simulating fluid dynamics and is typically solved using numerical methods.

5.2 Solid Motion Equations (Lagrangian Equations):

In the Lagrangian coordinate system, the motion of the solid is typically described using elastic mechanics or other solid dynamics models (Noh,1964). The basic equation for solid motion can be written as:

Motion equation:

$$\rho_s \frac{d^2\mathbf{u}_s}{dt^2} = \nabla\cdot\sigma_s + \rho_s\mathbf{g} \tag{7}$$

Here, ρ_s is the density of the solid, $\mathbf{u}_s$ is the displacement vector of the solid, σ_s is the stress tensor of the solid, and $\mathbf{g}$ is the gravitational acceleration vector.

Specifically, in the case of an elastic body, the elastic stress tensor σ_s can be obtained from the elastic strain tensor ε_s and the elastic modulus E relationship:

$$\sigma_s = E\cdot\varepsilon_s \tag{8}$$

Here, ε_s represents the elastic strain tensor. For linear elastic materials, the relationship between the elastic strain tensor and displacement is:

$$\varepsilon_s = \frac{1}{2}(\nabla\mathbf{u}_s + (\nabla\mathbf{u}_s)^T) \tag{9}$$

Here, u_s is the displacement vector of the solid, and $(\nabla\mathbf{u}_s)^T$ is the transpose of the displacement gradient.

Therefore, combining the above two equations, the relationship between the shear

stress tensor and displacement is given by:

$$\sigma_s = E \cdot \varepsilon_s = E \cdot \left(\frac{1}{2}(\nabla \mathbf{u}_s + (\nabla \mathbf{u}_s)^{\mathrm{T}})\right) \tag{10}$$

This relationship is used to describe the elastic behavior of solids and is typically employed in the Eulerian-Lagrangian method for modeling solids.

When the expression for the elastic stress tensor (10) is substituted into the solid's motion equation (7), the elastic equation describing the motion of the solid can be obtained. In the Lagrangian coordinate system, the elastic equation is typically written in the following form:

$$\rho_s \frac{d^2 \mathbf{u}_s}{dt^2} = \nabla \cdot \left(E \cdot \left(\frac{1}{2}(\nabla \mathbf{u}_s + (\nabla \mathbf{u}_s)^{\mathrm{T}})\right)\right) + \rho_s \mathbf{g} \tag{11}$$

Here, ρ_s is the density of the solid, $\mathbf{u}_s$ is the displacement vector of the solid, E is the elastic modulus.

The above equation describes the motion of the solid under external forces and gravity, where the elastic term reflects the elastic properties of the material. It is important to note that this equation is based on linear elastic theory, and for nonlinear and large deformation cases, one may need to consider the material's nonlinear behavior, such as using more complex material models like nonlinear elastic or plastic models.

5.3 CEL Method

As illustrated in Fig.S6, the solution process of the Euler equations is divided into two steps. Initially, in the Lagrangian solving step, the grid is bound to the material and undergoes deformation. Subsequently, the Euler solving step is executed, remapping the grid back to the initial grid corresponding to the spatial initial position. In this step, the positions of materials and material boundaries in each initial grid are defined. The Euler solving step is also referred to as the remapping step.

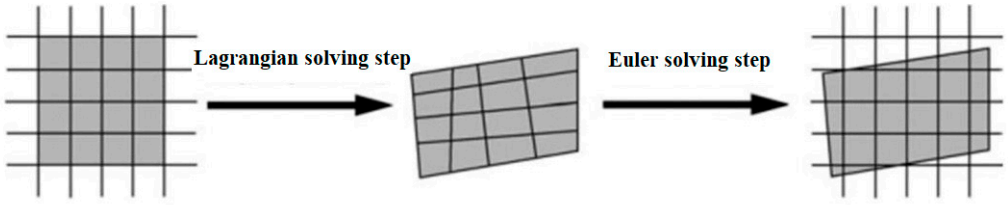

Figure S6. The schematic diagram of operator splitting for the Euler equations

In the ABAQUS/Explicit module, the Volume of Fluid (VOF) method is employed for solving the Euler step. The VOF method, introduced by (Hirt et al. 1981), is applicable in the context of Eulerian finite element methods for describing the position and shape of material boundaries. It supports the imposition of displacement or velocity boundary conditions directly from Lagrangian bodies to Eulerian bodies in

the CEL method.

In the case of a single-phase problem, a field function is defined as$\phi(x,t)$. For any point in the solution domain, when the material occupies that point, $\phi(x,t)=1$; conversely, when the point is empty, $\phi(x,t)=0$. For grids containing material boundaries, the average value of the function within the grid is denoted as $\bar{\phi}$, representing the volume fraction of material in the grid. Accordingly, $\bar{\phi}=1$ indicates that the grid is filled with material, while $\bar{\phi}=0$ signifies that the grid is empty, indicating the absence of material boundaries within the grid.

The VOF method efficiently constructs material boundaries using only the volume fraction parameter within the grid, making it a highly effective Euler remapping method.

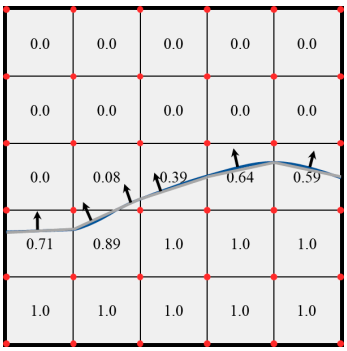

Figure S7. The Volume of Fluid method involves the representation of material volume fraction and the schematic diagram of material boundaries

As shown in the Fig.S7, when the material volume fraction within the grid is known, the position of material boundaries within the grid can be further determined. The material boundary, with respect to the function $\phi(x,t)$, represents an iso-surface, indicating that the gradient direction on the material boundary ϕ should be perpendicular to it. When both $\bar{\phi}$ the volume fraction and ϕ the average gradient direction within the grid are known, a line can be defined within the grid, as illustrated by the gray line in Fig.S7, serving as a rough representation of the material boundary. After connecting material boundaries in adjacent grids, other methods, such as the use of Bézier curves in ABAQUS/Explicit, are employed for smoothing the rough boundaries, as shown by the blue curve in Fig.S7.

6 Cable force time-history curves

We provide the tension time-history curves of the cable under various conditions to further illustrate the dynamic changes in tension. We found that the cable enters a failure state when the seismic wave peak acceleration is greater than or equal to 0.05g, as shown in Fig.S8. In addition, we found that the cable force fluctuated most obviously under the action of 11hz sine wave, as shown in Fig.S9.

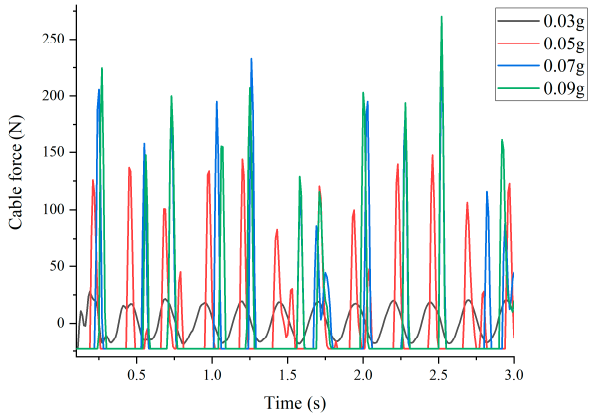

Figure S8. Variation curve of cable tension under the action of sinusoidal waves with different peak accelerations

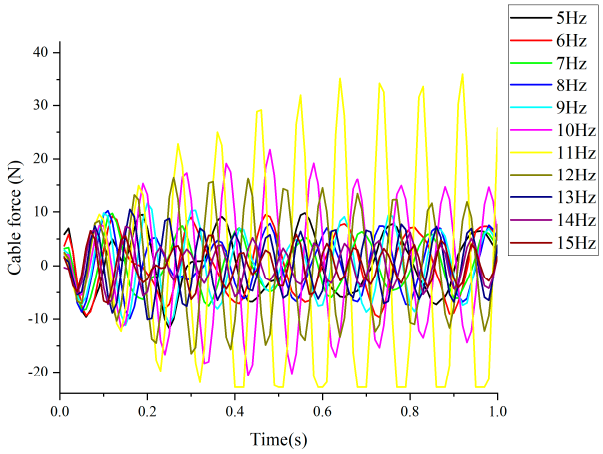

Figure S9. Variation curve of cable tension under the action of sinusoidal waves with different frequencies

References

Sun, S., CHEN J. 2008. Dynamic response analysis of SFT. Dalian University of Technology, Dalian. (in Chinese)

CHEN J, LI J., SUN S.2012.Experimental and numerical analysis of submerged floating tunnel J. Cent. South Univ.19: 2949−2957

Xiaoshize. 2020.Research on constitutive model and numerical simulation of sand rheology under low effective stress. Tsinghua University,Beijing.(in Chinese)

Hirt C W, Nichols B D . 1981 Volume of fluid (VOF) method for the dynamics of free boundaries. Journal of Computational Physics, 39(1):201 -225.